JOURNAL OF AIRCRAFT
Vol. 30, No. 4, July–Aug. 1993

Static Aeroelastic Control of an Adaptive Lifting Surface

S. M. Ehlers*
McDonnell Douglas Technologies, Inc., San Diego, California 92127
and
T. A. Weisshaar†
Purdue University, West Lafayette, Indiana 47907

This article examines the ability of an active material to change lift by changing the static aeroelastic stiffness of swept and unswept wings. Piezoelectric actuators are embedded in an idealized laminated composite wing structure that can adapt to changing flight conditions. A feedback control system senses wing root strains and then applies a proportional voltage to active actuator layers to change wing lift or divergence dynamic pressure. The amount of wing lift change is constrained by limited piezoelectric stiffness, electromechanical coupling coefficients, and limits on the size of the applied electric field. It is also constrained by the way the active material is integrated into the parent structure. Nondimensional parameters identify these limits by relating wing parameters to active material capabilities.

Introduction

THE central focus of this article is an examination of the suitability and limits of active materials when used to increase or decrease lift on a wing. This task requires the identification of the relationship between this design goal and the material properties of active material actuator elements. Usually material properties are either prescribed when the design process begins, or choices are so limited that materials immediately become active constraints to the design process. The introduction of active or smart materials may change this, particularly where aeroelastic design goals are concerned.

The term "smart materials" describes active materials that adapt on command to changing design conditions. Active materials respond to commanded, controlled external stimuli such as an electric field, a magnetic field, or heat. The adaptive structural response can be a change in stiffness or a change in the dimensions of the material. The size of the applied stimuli is actively controlled and its effect on the structure is monitored so that the stiffness and shape of the structure are controlled.

Proposed engineering uses of active materials, such as piezoelectric ceramics, range from active control of underwater structural vibrations to the active damping of vibrations of precision structures in space. The formulation of control laws to activate the materials controlling structural response and to determine their placement within the structural design is an essential part of this technology. As a result, issues such as the best control law or the most effective placement of the actuator material must be considered, although the present study does not address these issues in depth.

Changing the shape of an aircraft wing, even slightly, will change the aerodynamic loads. The study of the interaction between aerodynamic loads and structural deflections is called aeroelasticity. Because aerodynamic forces, like structural forces, depend on displacement, the apparent stiffness of the wing changes as airspeed increases. This stiffness change will affect the distribution and size of the aerodynamic loads.

Presented as Paper 90-1078 at the AIAA/ASME/ASCE/AHS/ASC 31st Structures, Structural Dynamics and Materials Conference, Long Beach, CA, April 2–4, 1990; received Jan. 24, 1991; revision received March 15, 1992; accepted for publication May 5, 1992.

*Manager, Advanced Concepts. Senior Member AIAA.
†Professor, School of Aeronautics and Astronautics. Associate Fellow AIAA.

If the aerodynamic force on a wing is increased because of aeroelastic interaction, the surface is said to have increased lift effectiveness and the wing is called a "wash-in" wing. Any increase in aerodynamic forces created by aeroelastic effects can be reduced by decreasing the aircraft angle of attack. On the other hand, an increase in aerodynamic force may be used to maneuver the aircraft without changing its attitude.

This article discusses how active materials may be used to change the aeroelastic stiffness of wings. A change in apparent stiffness will either increase or decrease the aerodynamic forces to maneuver the aircraft or to change the static aeroelastic stability of the wing. This investigation will show that the ability of active materials to control wings is limited by wing size and the current state of materials technology. Three cases of active control are considered: 1) an unswept wing with only torsional deformation included; 2) a swept wing with only bending permitted; and 3) a swept wing with advanced composite material construction and bend/twist coupled deformation. In each case we will identify limits of active control of loads and relate these limits to material properties and geometric parameters.

Active Materials

Active materials considered for structural shape control include piezoelectrics,[1] electrostrictors,[2,3] magnetostrictors,[4,5] shape memory effect materials (SME),[6,7] and electrorheological fluids.[8,9] The use of thermomechanical coupling to control structural shape has also been explored.[10–12] Optical fibers are also included in this group because of their exceptional capabilities as sensors.[13,14]

An electric charge is produced when a piezoelectric material is subjected to a mechanical stress. As a result they can be used as sensors. Conversely, the material will strain when an electric field is applied to a piezoelectric element so that they can be used to create an actuator.[1,15]

This study will focus exclusively on piezoelectric actuators. While piezoelectrics can be cast into many forms, the actuators used in this article are thin layers of material embedded in a beam structure, as shown in Fig. 1. The upper and lower surfaces of the material layer are conductively coated to form electrodes, across which a voltage V_k is applied to create an electric field $E_3 = V_k/t_k$ in Fig. 1. Electromechanical coupling in the piezoelectric material between the transverse electric field (E_3) and the inplane normal strains is important. Two constants of proportionality, denoted as d_{31} and d_{32}, give the strain in the 1 and 2 directions in Fig. 1 due to a unit electric field in the transverse (3) direction.

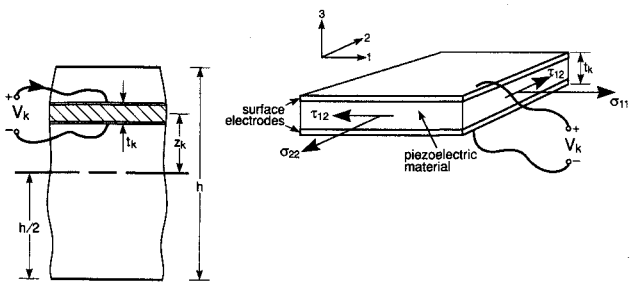

Fig. 1 Piezoelectric actuator layer and position within beam cross section.

Table 1 Piezoelectric material properties

Property	PVDF	PZT
d_{31}, in./V	0.91×10^{-9}	-6.54×10^{-9}
d_{32}, in./V	0.12×10^{-9}	-6.54×10^{-9}
E_3^*, V/in.	0.25×10^6	0.015×10^6
$E_{11}d_{31}E_3^*$, psi	66.0	893.0
$E_{11}d_{31}E_3^*/\rho$, in.	1020.0	3210.0

The effectiveness of piezoelectric actuator is determined by 1) the size of the d_{31} and d_{32} coefficients; 2) its stiffness or Young's modulus in the 1 and 2 directions; and 3) limits on the magnitude of the applied field. A critical limitation of piezoelectric materials in the maximum electric field that may be applied without depoling the piezoelectric. The positive and negative field limits are usually unequal,[16] but for this study they will be assumed to be equal and are denoted by E_3^*.

There are two candidate piezoelectric materials for aeroelastic actuators. PZT is a piezoelectric ceramic, or piezoceramic, which is transversely isotropic in the layer plane. Its modulus of elasticity is comparable to that of aluminum, whereas, its density is comparable to steel. Unfortunately, PZT is a brittle material with low ultimate strain. PVDF is a piezoelectric polymer, or piezopolymer. It has a modulus of elasticity about 3% of aluminum and density of about 65% of aluminum.

The elastic constants, electrical and coupling properties, and density of the two most common piezoelectric materials, PZT and PVDF, are presented in Table 1. Two important measures of actuator effectiveness appear in Table 1. These are the actuator strength, given as the product of piezoelectric modulus E_{11}, times piezoelectric strain d_{31}, times the maximum field E_3^*, and actuator strength per unit weight $E_{11}d_{31}E_3^*/\rho$.

Additional features of piezoelectric materials to be considered in the design of adaptive structures include nonlinear behavior, hysteresis, and aging problems. However, for this study, these effects will be neglected so that we may concentrate on the control of static aeroelastic loads. This study will assume linearity between the applied field and the piezoelectric strain.

Active Static Aeroelasticity

Static aeroelasticity concerns itself with the interaction between flight vehicle structural displacement and aerodynamic loads. Static aeroelastic effects not only influence flight performance within the operational envelope, but also affect structural integrity, stability, and control surface effectiveness.[17]

Static aeroelastic analysis must relate external loads, including aerodynamic and disturbance loads, to the internal elastic structural loads. An adaptive structure must include a set of displacement-dependent control forces, either internal to the structure or external to it. Both the control forces and aerodynamic loads are functions of a set of generalized coordinates or displacements, ξ.

The general form of the controlled aeroelastic static equilibrium equation is given by

$$S(\xi) - C(\xi) - A(q, \xi) = Q_d \tag{1}$$

S, A, and C are the structural, aerodynamic, and control force operators, respectively, that define the generalized forces as functions of the generalized displacements. The aerodynamic operator is also a function of flight dynamic pressure, represented as q. These operators can be matrices or differential operators.

If the external load Q_d is set to zero, Eq. (1) defines the neutral static stability condition of the system. When the structural, aerodynamic, and control operators are grouped together, they form an adaptive aeroelastic stiffness operator. The eigenvalues (q) determine the static instability dynamic pressures or divergence condition for the wing. As a result, changes in the control law or the aerodynamic forces can change the effective stiffness of the lifting surface, the size of the generalized displacements, the aerodynamic loads, and the stability of the wing.

The relation between the control forces and generalized displacements is determined by a control law. The control law describes a mathematical relation between actuator forces and sensor outputs. The sensors may be strain gauges, displacement gauges, optical fibers, or angle-of-attack probes. In the most general case, the lifting surface may be divided into multiple spanwise segments of sensors and actuators which are not necessarily located at the same points on the structure. The addition of active structural elements to the wing will change both $S(\xi)$ and $C(\xi)$.

Several previous studies have suggested the use of adaptive materials for aerodynamic load modification. Crawley et al.[18] were the first to suggest and examine the use of piezoelectric materials to change camber and twist of a low-aspect ratio surface. The aeroelastic interaction of these deformations with airloads was not included. These studies were followed by an examination of static aeroelastic control of such surfaces.[19] More recently, a study by Ehlers[20] investigated the use of adaptive material control of static aeroelastic effects such as divergence and roll effectiveness. In addition, a recent investigation by Song et al.[21] examined imbedded piezoelectric actuators in a thin-wall structure to control static wing divergence.

Wing Adaptive Structure

The wing structure used in this study is idealized as a laminated beam with bending and torsion deformation freedom. Chordwise (camber) deformations are ignored, consistent with the behavior of moderate to high-aspect ratio wings with a stiff rib structure. The structural cross section of the idealization is shown in Fig. 2. It will also be assumed that the piezoelectric materials can be integrated into the wing structure so that they can provide both bending and torsion actuation. This assumption has limits that are to be addressed later.

The relations between the beam internal cross-sectional bending moment M, torque T, bending slope ϕ, and twist rate θ', have the following form:

$$\begin{Bmatrix} M \\ T \end{Bmatrix} = \begin{bmatrix} EI & -K \\ -K & GJ \end{bmatrix} \left(\begin{Bmatrix} \phi' \\ \theta' \end{Bmatrix} - \begin{Bmatrix} \Gamma_\phi \\ \Gamma_\theta \end{Bmatrix} E_3 \right) \tag{2}$$

where $(\,)'$ denotes differentiation with respect to the beam spanwise coordinate y shown in Fig. 3. The beam bending, torsion, and bend/twist coupling cross-sectional stiffnesses are denoted by EI, GJ, and K, respectively. The stiffness of embedded actuator layers is also included in EI, GJ, and K. The electric field is proportional to the voltage applied and inversely proportional to the thickness of the actuator.

The piezoelectric actuators create wing curvature (ϕ') and twist rate (θ'). The coefficients Γ_ϕ and Γ_θ represent the bend-

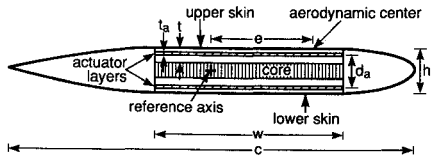

Fig. 2 Idealized adaptive wing structural cross section.

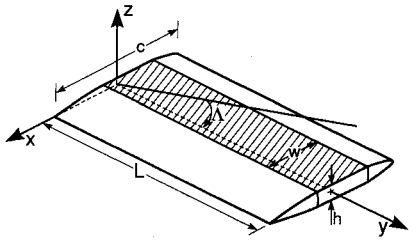

Fig. 3 Uniform wing planform, showing wing box dimensions and sweep angle with respect to airflow.

ing curvature and twist rate per unit electric field. These piezoelectric actuation coefficients may be approximated by the following relationships[20]:

$$\Gamma_\phi = [(GJe_{3x} + Ke_{3s})/(EI \cdot GJ - K^2)](t_a d_a w) \quad (3)$$

$$\Gamma_\theta = [(Ke_{3x} + EIe_{3s})/(EI \cdot GJ - K^2)](t_a d_a w) \quad (4)$$

The dimensions t_a, d_a, and w are shown in Fig. 2.

The piezoelectric parameters e_{3x} and e_{3s} in Eqs. (3) and (4) are related to the piezoelectric strain coefficients d_{31} and d_{32} as follows. The plane stress constitutive relations for a thin layer of isotropic or orthotropic piezoelectric material with a transversely applied electric in the material coordinate system are given by

$$\begin{Bmatrix} \sigma_{11} \\ \sigma_{22} \\ \tau_{12} \end{Bmatrix} = \begin{bmatrix} Q_{11} & Q_{12} & 0 \\ Q_{12} & Q_{22} & 0 \\ 0 & 0 & Q_{66} \end{bmatrix} \left(\begin{Bmatrix} \varepsilon_{11} \\ \varepsilon_{22} \\ \gamma_{12} \end{Bmatrix} - \begin{Bmatrix} d_{31} \\ d_{32} \\ d_{36} \end{Bmatrix} E_3 \right) \quad (5)$$

where Q_{ij} represent elastic coefficients of an orthotropic (or isotropic) material.[22] Shear strain per unit field is given by d_{36}, which is zero for currently available piezoelectric materials.

The active material axes are not necessarily aligned with the wing x-y reference axes in Fig. 3. If the piezoelectric element is rotated with respect to the structural reference axis shown in Fig. 3, the constitutive relations become

$$\begin{Bmatrix} \sigma_{xx} \\ \sigma_{yy} \\ \tau_{xy} \end{Bmatrix} = \begin{bmatrix} Q_{xx} & Q_{xy} & Q_{xs} \\ Q_{xy} & Q_{yy} & Q_{ys} \\ Q_{xs} & Q_{ys} & Q_{ss} \end{bmatrix} \left(\begin{Bmatrix} \varepsilon_{xx} \\ \varepsilon_{yy} \\ \gamma_{xy} \end{Bmatrix} - \begin{Bmatrix} d_{3x} \\ d_{3y} \\ d_{3s} \end{Bmatrix} E_3 \right) \quad (6)$$

For the transformed constitutive relations, the piezoelectric shear strain coefficient d_{3s} is nonzero only when d_{31} and d_{32} are unequal, or when extension-shear coupling is present. The piezoelectric stress coefficients e_{3x}, e_{3y}, and e_{3s} are defined as the product of the piezoelectric elastic constants and the strain coefficients:

$$\begin{Bmatrix} e_{3x} \\ e_{3y} \\ e_{3s} \end{Bmatrix} = \begin{bmatrix} Q_{xx} & Q_{xy} & Q_{xs} \\ Q_{xy} & Q_{yy} & Q_{ys} \\ Q_{xs} & Q_{ys} & Q_{ss} \end{bmatrix} \begin{Bmatrix} d_{3x} \\ d_{3y} \\ d_{3s} \end{Bmatrix} \quad (7)$$

The coefficients e_{3x}, e_{3y}, and e_{3s} give the chordwise, spanwise, and in-plane shear stresses per unit field for the layer. Equations (3), (4), and (7) indicate that a large combination of Q_{11} and d_{31} is required for an effective, strong actuator.

Unless the designer is creative, the value of e_{3s} will be zero. In general, e_{3x} will be equal approximately to $Q_{11}d_{31}$ for an actuator strip such as that shown in Fig. 3. On the other hand, schemes for directional control to provide an effective value of e_{3s} have been demonstrated. In particular, the directionally attached piezoelectric (DAP) concept proposed by Barrett[23] offers the promise of creating anisotropic piezoelectric effects with isotropic piezoelectric materials.

The adaptive wing model is shown in Fig. 3 with the piezoelectric actuator sheet shown shaded. The wing can be swept at an angle Λ to the flow. The wing box has chord w and depth h.

Control of an Unswept Wing

Three types of static aeroelastic control models will be examined, as previously mentioned. The first is a uniform property wing without bending-torsion coupling and sweep angle Λ equal to zero. The wing idealization is clamped at the wing root at an angle-of-attack θ_0 with respect to the airflow. The wing loads are idealized with strip theory aerodynamics.[24] The governing static equilibrium differential equation, in terms of the nondimensional spanwise coordinate $\eta = y/L$, reduces to[24]

$$\theta'' + \lambda^2\theta = -\lambda^2\theta_0 \quad (8)$$

where $(\,)'$ denotes differentiation with respect to η and

$$\lambda^2 = q(ceL^2/GJ)a_0 \quad (9)$$

In Eq. (9), q is the dynamic pressure, while a_0 is the section lift curve slope. The clamped wing root boundary condition requires that

$$\theta(0) = 0 \quad (10)$$

The inclusion of the piezoelectric actuators enters as a boundary condition that requires the net torque to vanish at the wing tip. This boundary condition, using the torsion relation in Eq. (2) is written as

$$T(1) = GJ[\theta'(1) - \Gamma_\theta E_3 L] = 0 \quad (11)$$

or

$$\theta'(1) = \Gamma_\theta E_3 L \quad (12)$$

Notice, from Eq. (4), that we require a torsional actuator with an effective nonzero value of e_{3s}.

This wing is now active, but not adaptive. This latter feature is introduced by requiring that the applied electric field E_3 be proportional to the wing root torque or twist rate $\theta'(0)$. The result is

$$E_3 = k\theta'(0) \quad (13)$$

or

$$\theta'(1) = \Gamma_\theta kL\theta'(0) = K_p\theta'(0) \quad (14)$$

where k and K_p are gains specified by the control/structural designer. The solution for the twist of this wing is

$$\theta(\eta) = \{[\sin\lambda/(\cos\lambda - K_p)]\sin\lambda\eta + \cos\lambda\eta - 1\}\theta_0 \quad (15)$$

The twist of the lifting surface depends on the dynamic pressure parameter λ, and may be controlled by the proper choice of k and K_p. Note that K_p appears as an independent parameter, but it is related to E_3 by Eqs. (13) and (14).

Lift Effectiveness and Divergence

The twist $\theta(\eta)$ and the lift on the adaptive structure depend on the gain parameter K_p and the piezoelectric material, as indicated in Eqs. (13) and (14). The wing lift effectiveness is defined as the ratio of lift on the active wing L_f, to lift on a rigid wing L_r, at the same angle of attack θ_0. This ratio is computed by integrating the angle of attack distribution in

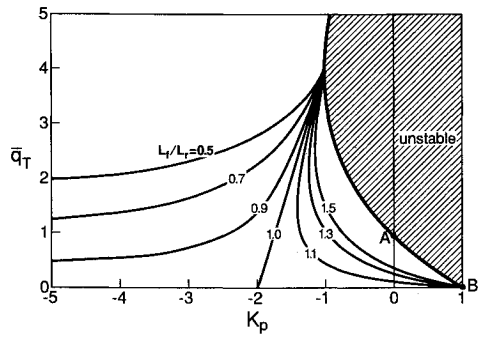

Fig. 4 Contours of constant unswept adaptive wing lift effectiveness as a function of $\bar{q}_T$ and K_p.

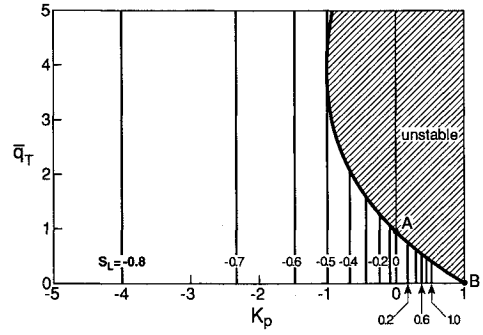

Fig. 5 Contours of required unswept adaptive wing actuator strength parameter S_L as a function of $\bar{q}_T$ and K_p.

Eq. (15) to compute the total wing lift. This ratio is

$$(L_f/L_r) = \{[(\sin\lambda(1 - K_p)]/[\lambda(\cos\lambda - K_p)]\} \quad (16)$$

Divergence occurs when L_f grows without bound. From Eq. (16), this occurs when

$$\cos\lambda = K_p \quad (17)$$

A normalized nondimensional dynamic pressure is defined as

$$\bar{q}_T = \lambda^2/\lambda_0^2 \quad (18)$$

where λ_0^2 is equal to $\pi^2/4$, the divergence dynamic pressure of an ordinary unswept wing.

The wing divergence boundary and contours of constant lift effectiveness are plotted in Fig. 4 as a function of $\bar{q}_T$ and K_p. Figure 4 indicates that an adaptive structure can increase the divergence dynamic pressure and change lift effectiveness. Point A locates the passive wing divergence condition. When K_p equals 1, the wing is statically unstable, even without an airstream, as indicated by point B in Fig. 4.

At a constant value of K_p, an increase in dynamic pressure will increase the lift effectiveness and the lift per angle of attack θ_0. On the other hand, if we choose $\bar{q}_T$ equal to 1 and let K_p range from 0 to -4, the lift effectiveness (and lift at a fixed angle of attack) declines. As a result, we can increase or decrease aircraft altitude by simply changing K_p. However, limitations of the piezoelectric material properties and its position in the laminate cross section impose limits on the maximum value of K_p. These limitations will now be considered.

Actuator Strength and Control Limits

Limits on the maximum field for the piezoelectric, denoted by E_3^*, limit the twist rate that may be commanded by the control system. As indicated by Eqs. (4) and (12), this limit depends on the material, its location in the structural cross section, and the size of the lifting surface.

A nondimensional parameter S_0 is derived using Eqs. (13–15) to measure the piezoelectric actuator effectiveness or strength at different dynamic pressures. The actuator strength is defined as the commanded tip twist, when the aerodynamic loads are not present, divided by the initial wing root angle. This parameter, denoted as S_0, is

$$S_0 = (\Gamma_\theta E_3 L/\theta_0) \quad (19)$$

With the aerodynamic loads applied, Eqs. (12), (14), and (15) may be used to compute the numerator in Eq. (19). This gives us

$$S_0 = (\Gamma_\theta E_3 L/\theta_0) = [K_p\lambda \sin\lambda/(\cos\lambda - K_p)] \quad (20)$$

This computation assumes that the wing root angle of attack is fixed, such as will occur in a wind-tunnel test.

Equation (19) computes the amount of actuator strength available, normalized with respect to the wing root incidence angle. Equation (20) shows this available actuator strength equated to the actuator strength required to generate the values of control gain K_p. Note that, by definition, the actuator strength available is independent of dynamic pressure, while the amount required depends in general on λ and K_p (and the control law).

A similar actuator effectiveness or strength parameter may also be derived when the wing is in free flight. S_L is the ratio of the tip twist due to the actuator, to the wing tip twist due to aerodynamic loads in 1-g flight. The difference between the fixed wing root condition and a trimmed vehicle in free flight, is that the wing lift in trimmed flight is constant, while θ_0 changes with dynamic pressure.

The wing root angle θ_0, required to make lift equal to aircraft weight, is proportional to aircraft weight W. Solving for θ_0 in terms of aircraft weight W

$$\theta_0 = (W/qSa_0)\{[\lambda(\cos\lambda - K_p)]/[\sin\lambda(1 - K_p)]\} \quad (21)$$

When we substitute this relationship and that for Γ_θ into Eq. (19), we have the available actuator strength as

$$S_L = \frac{\Gamma_\theta E_3 L}{\frac{1}{2}(WeL/GJ)} = 4\frac{(e_{3s}E_3)(t_a/h)(d_a/h)(w/c)(h/c)^2}{(W/S)(e/c)(L/c)} \quad (22)$$

where S is the surface area of the wing and the other geometric parameters are defined in Figs. 2 and 3.

The required value of S_L is expressed in terms of K_p by substituting $\theta(\eta)$ into Eq. (14). This gives

$$S_L = [K_p\theta'(0)/\theta_0] = [K_p/(1 - K_p)] \quad (23)$$

Equating the actuator strength available to the actuator strength required

$$e_{3s}E_3 = \frac{1}{4}\left(\frac{K_p}{1 - K_p}\right)\frac{(W/S)(e/c)(L/c)}{(t_a/h)(d_a/h)(w/c)(h/c)^2} \quad (24)$$

This equation shows that we cannot choose values of K_p and wing parameters without regard to piezoelectric material properties.

Contours of the required constant lift strength parameter [Eq. (23)] are shown in Fig. 5. As K_p is increased from zero, the required value of S_L must increase. Therefore, the available value of S_L given in Eq. (22) limits the size of lift change. The contours of required S_L in Fig. 5 can be overlaid on the lift effectiveness contours in Fig. 4 to determine the required actuator strength for a given value of wing lift. Notice that, at larger values of $\bar{q}_T$, only small changes in S_L are required to change the lift by significant amounts.

Pure Bending Deformation

Bending deflection of a swept wing changes wing aerodynamic loads.[24] Aeroelastic interaction between bending and aerodynamic forces is isolated by considering a swept uniform wing with torsion excluded. For the wing shown in Fig. 3,

when Λ is not zero, beam bending theory and strip theory aerodynamics result in the following static equilibrium equation, in terms of the bending slope ϕ:

$$\phi''' + \mu^3\phi = \mu^3(\theta_0/\tan\Lambda) \tag{25}$$

where $(\,)'$ denotes differentiation with respect to $\eta = y/L$. The initial angle θ_0 is measured with respect to the y axis in Fig. 3. The aeroelastic nondimensional dynamic pressure parameter μ is defined by the relation

$$\mu^3 = q(cL^3/EI)a_0 \sin\Lambda\cos\Lambda \tag{26}$$

Note that μ is negative for swept-forward wings. The wing cantilever root requirement and the vanishing of transverse shear at the wing tip create two boundary conditions:

$$\phi(0) = 0 \tag{27}$$

$$\phi''(1) = 0 \tag{28}$$

The third boundary condition is a bending moment condition at the tip, written as

$$\Gamma_\phi E_3 L = \phi'(1) \tag{29}$$

We can relate the applied field E_3 on the piezoelectric layers to the bending curvature at the wing root with a control law as follows:

$$\phi'(1) = K_p\phi'(0) \tag{30}$$

A closed-form solution to Eq. (25) with its associated boundary conditions provides the wing bending slope as a function of μ, θ_0, and K_p. Static aeroelastic wing divergence boundaries and lift effectiveness are then computed. This wing will diverge only if swept forward ($\Lambda < 0$).

The normalized dynamic pressure $\bar{q}_B$ is the ratio of μ^3 to the wing divergence value μ_0^3 (-6.33) for a nonadaptive swept wing. Positive values of $\bar{q}_B$ are associated with a forward-swept wing while negative values indicate aft-wing sweep. Contours of swept wing lift effectiveness as a function of $\bar{q}_B$ and K_p are presented in Fig. 6. Figure 6 is similar to Fig. 4, except that there are two regions of instability for the swept wing.

In Fig. 6 the stability boundary for the forward-swept wing passes through points A and B. Like the unswept wing, point A is the divergence dynamic pressure of a nonadaptive wing while point B is the self-excited wing static instability at zero airspeed. Figure 6 shows the extent to which the lift effectiveness of both forward- and aft-swept wings may be changed if only the appropriate values of K_p can be attained. Note that there is a combination of K_p and dynamic pressure can maintain rigid wing lift effectiveness ($L_f/L_r = 1.0$) so that the wing deforms, but the lift is unchanged. In addition, when $\bar{q}_B$ is zero, bending has no effect on unswept wing lift so L_f/L_r is 1.

The bending actuator creates an effective angle of attack equal to $-\phi\tan\Lambda$. In this case, the available fixed root wing actuator strength parameter for pure bending is defined as

$$S_0 = -(\Gamma_\phi E_3 L\tan\Lambda/\theta_0) \tag{31}$$

The expression for the constant lift actuator strength parameter S_L is found by solving for θ_0 in terms of aircraft weight W and bending stiffness. Substituting this value of θ_0 into Eq. (31), together with appropriate expressions for Γ_θ and EI, the constant lift actuator strength available is

$$S_L = -4\frac{(e_{3x}E_3)(t_a/h)(d_a/h)(h/c)^2(w/c)}{(W/S)(L/c)^2} \tag{32}$$

The value of S_L required is found using Eqs. (29) and (30). Contours of S_L required are plotted against $\bar{q}_B$ and K_p in Fig. 7. When overlaid on Fig. 6, these S_L contours show that the

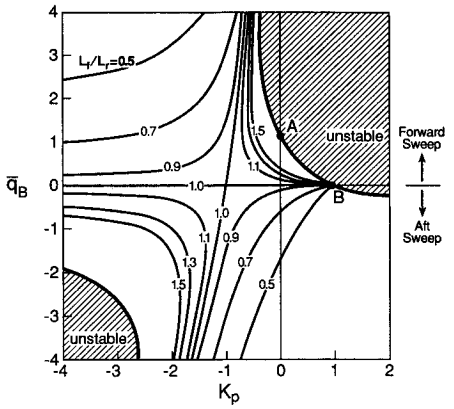

Fig. 6 Contours of lift effectiveness for an adaptive swept wing with bending only, as a function of $\bar{q}_B$ and K_p.

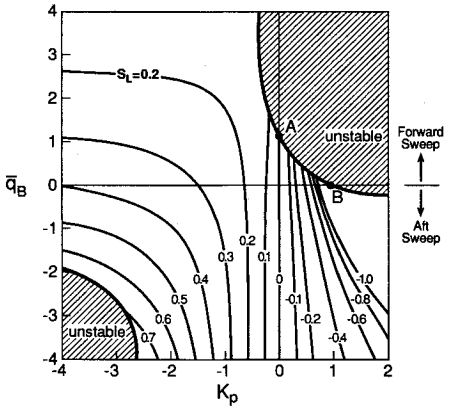

Fig. 7 Contours of required swept wing, bending only actuator strength parameter S_L as a function of $\bar{q}_B$ and K_p.

ability of the adaptive structure to change lift wing is increased when the dynamic pressure is relatively high. Then, small changes in stiffness create large changes in aerodynamic loads.

The required S_L to decrease lift and lift effectiveness on a forward-swept wing ($\bar{q}_B > 0$) decreases rapidly when dynamic pressure increases. On an aft swept wing, S_L required to reduce the lift effectiveness also decreases with increasing dynamic pressure, although the decrease is less than for the forward-swept wing.

Swept Wing with Bending and Torsion Freedom

Although the previous case represents a limiting case, lift distribution on a swept wing depends on both bending and torsion deformation. The static equilibrium equations for the uniform wing advanced composite beam model with strip theory aerodynamics are[20,25]

$$GJ\theta'' - K\phi'' = qceL^2a_0(\theta_0 + \theta - \phi\tan\Lambda) \tag{33}$$

$$EI\phi''' - K\theta''' = qcL^3a_0(\theta_0 + \theta - \phi\tan\Lambda) \tag{34}$$

These equations may be combined into a single equation by transforming θ and ϕ into a single variable. This term, α_e, the effective angle of attack of a chordwise wing section, is given by

$$\alpha_e = \theta - \phi\tan\Lambda \tag{35}$$

Equations (33) and (34) then read

$$\alpha_e''' + A\alpha_e' + D\alpha_e = -D\theta_0 \tag{36}$$

The nondimensional constants A and D are

$$A = q\frac{ceL^2}{GJ}a_0\cos^2\Lambda\left[\frac{1 - (K/EI)\tan\Lambda}{1 - K^2/(EIGJ)}\right] \tag{37}$$

$$D = q\frac{cL^3}{EI}a_0\cos^2\Lambda\left[\frac{\tan\Lambda - (K/GJ)}{1 - K^2/(EIGJ)}\right] \tag{38}$$

In the case of pure torsional deformation, D is zero while A reduces to λ^2. For pure bending deformation, A is zero and D reduces to μ^3.

The boundary conditions due to the cantilever wing root and vanishing transverse shear at the wing tip are

$$\alpha_e(0) = 0 \tag{39}$$

$$\alpha_e''(1) + A\alpha_e(1) = -A\theta_0 \tag{40}$$

At the wing tip, both the internal bending moment and torque are zero. These two conditions involve the piezoelectric actuator and combine to yield

$$\alpha_e'(1) = (\Gamma_\theta - \Gamma_\phi \tan\Lambda)E_3L \tag{41}$$

The applied electric field must be related to a combination of bending and torsion deformation. A wide variety of choices are possible. Since α_e defines the displacement, sensing the same combination of twist rate and curvature that form α_e' seems appropriate. As a result, the following control law is used:

$$(\Gamma_\theta - \Gamma_\phi \tan\Lambda)E_3L = \alpha_e'(1) = K_p\alpha_e'(0) \tag{42}$$

The closed-form solution to these equations provides the aeroelastic lift on the wing and the divergence boundary.

Static aeroelastic stability of the swept adaptive wing depends on A, D, and the gain parameter K_p. In Fig. 8, the stability boundary for three values of the gain parameter is shown plotted against A and D. The region above each of these lines is a region of instability. This boundary pivots about a point in the first quadrant of Fig. 8 as K_p is increased or decreased. In addition the wing is stabilized if K_p is less than zero. The pivot point defines a wing configuration with A and D such that $\alpha_e'(0)$ is zero for any dynamic pressure.

The available fixed-root angle-of-attack actuator strength parameter S_0 for a swept wing with bending torsion-coupling is defined as

$$S_0 = \{[(\Gamma_\theta - \Gamma_\phi \tan\Lambda)E_3L]/\theta_0\} \tag{43}$$

The constant lift strength parameter S_L is found by substituting for θ_0 in terms of aircraft weight, stiffnesses, and geometric parameters. In terms of the vehicle geometric and performance parameters, stiffness, and piezoelectric material properties, the available S_L is given by

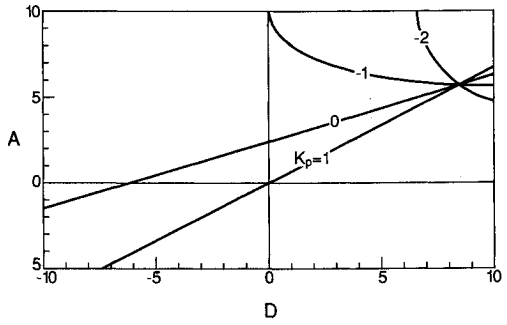

Fig. 8 Stability boundaries for a swept wing with bending and torsion deformation freedom at several values of K_p.

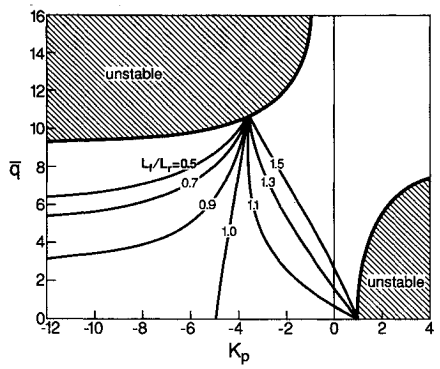

Fig. 9 Contours of constant lift effectiveness for a sweptback wing, A/D = 0.5.

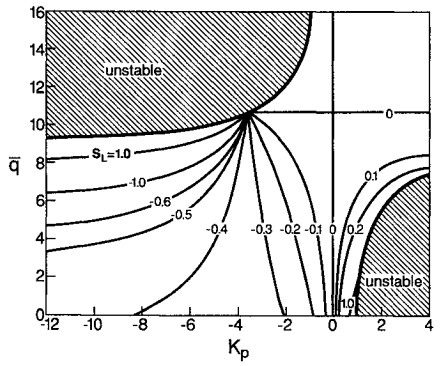

Fig. 10 Contours of required actuator strength S_L for the sweptback wing with A/D = 0.5.

$$S_L = 4\frac{[(K - GJ\tan\Lambda)e_{3x} + (EI - K\tan\Lambda)e_{3s}]E_3(t_a/h)(d_a/h)(w/c)(h/c)^2}{(W/S)(L/c)^2\sqrt{(e/c)^2(EI - K\tan\Lambda)^2 + (L/c)^2(K - GJ\tan\Lambda)^2}} \tag{44}$$

This expression may be simplified if K equals zero to become

$$S_L = 4\frac{\{e_{3s} - [(GJ/EI)\tan\Lambda]e_{3x}\}(t_a/h)(d_a/h)(w/c)(h/c)^2}{(W/S)(L/c)\sqrt{(e/c)^2 + (L/c)^2(GJ/EI)^2\tan^2\Lambda}} \tag{45}$$

Equation (45) reduces to Eq. (22) when the wing is unswept and has only torsion freedom and reduces to Eq. (32) for a swept wing with bending only.

To illustrate adaptive swept wing lift effectiveness control, consider two different wing configurations. The first has an A/D ratio of 0.5 to represent an aft-swept wing. This wing will not diverge if K_p is zero. Lift effectiveness contours for this wing are shown in Fig. 9, plotted as a function of K_p and nondimensional dynamic pressure $\bar{q}$, defined as

$$\bar{q} = \sqrt{A^2 + D^2} \tag{46}$$

Because the wing is swept back, D and A are always positive.

Two regions of instability appear in Fig. 9. One instability region occurs at low dynamic pressures with $K_p > 0$, while the other region occurs at higher dynamic pressures with $K_p < 0$. Like previous examples, the wing is unstable at zero airspeed with K_p is 1.

Contours of required S_L for this configuration are shown in Fig. 10. In general, the actuator strength parameter value required to change lift effectiveness decreases as dynamic pressure is increased.

The second example is a forward-swept wing where A/D is -1. Contours of constant lift effectiveness for this wing are shown in Fig. 11, plotted against $|\bar{q}|$ since $\bar{q}$ is always negative when $\Lambda < 0$. The divergence point for a wing without active control (K_p = 0) is at point A, while the control induced instability at zero airspeed is at point B. These contours resemble those in Fig. 4, plotted for the unswept wing.

Constant required lift strength parameter contours for the forward-swept wing are shown in Fig. 12. The active material actuator effort required to increase or decrease lift effective-

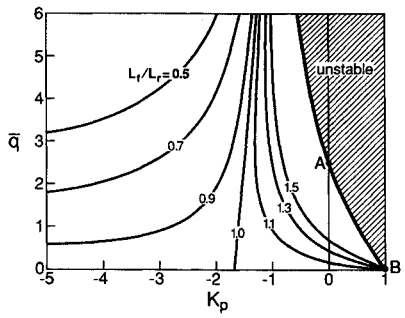

Fig. 11 Contours of lift effectiveness for a forward swept wing, $A/D = -1$.

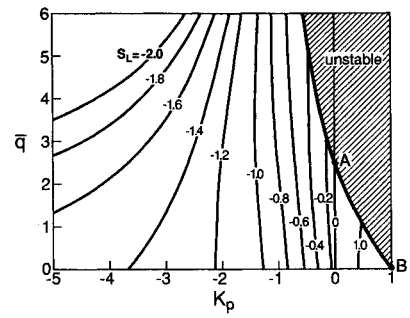

Fig. 12 Contours of constant actuator strength S_L for the forward swept wing with $A/D = -1$.

ness, decreases with dynamic pressure increases for a forward-swept wing. However, more actuator effort is required to decrease lift effectiveness than to increase it. Maintaining rigid wing lift ($L_F L_R = 1.0$) requires increasing actuator strength as airspeed increases because active materials must counteract the natural tendency of the flexible forward-swept wing to increase aerodynamic loads or "wash-in."

Conclusion

A laminated composite aeroelastic beam model with imbedded piezoelectric actuators has been used to study active control of lift and lift effectiveness. This control changes the constitutive relationship that controls the flexibility of the wing structure. The effectiveness of this concept depends upon actuator strength parameters derived in the study. These actuator effectiveness parameters are functions of wing geometry and the mechanical and piezoelectric properties of the materials used to control the wing shape.

The strength parameters indicate that available materials may fall short of the demands that are placed upon them. For instance, Eq. (24) indicates that the value of $e_{3s}E_s$ must increase linearly with wing loading (W/S), all other things being the same. Increases in vehicle size generally involve increased wing loading.

Equation (22) shows that available actuator strength is inversely proportional to the wing loading W/S. Since the aircraft weight is a function of volume (length cubed). While the wing area is a function of length squared, as aircraft size increases the actuator effectiveness declines inversely with length. This behavior appears due to a "square-cube law" phenomenon where the control necessary changes with the cube of the size of the vehicle, but the actuator area changes with the square of vehicle size.

Acknowledgments

T. A. Weisshaar acknowledges the support of NASA Grant NSG 1-157 and the efforts of the Technical Monitor, Jessica Woods-Vedeler.

References

[1]Crawley, E. F., and De Luis, J., "Use of Piezoelectric Actuators as Elements of Intelligent Structures," *AIAA Journal*, Vol. 25, No. 10, 1987, pp. 1373–1385.

[2]Uchino, K., and Nomura, S., "New Electromechanical Materials and Their Applications," *Japanese Journal of Applied Physics*, Vol. 21, Supplement 20-4, 1981, pp. 225–228.

[3]Newnham, R. E., Xu, Q. C., Kumar, S., and Cross, L. E., "Smart Ceramics," *Smart Materials, Structures and Mathematical Issues*, edited by C. A. Rogers, Technomic Publishing, Westport, CT, 1989, pp. 147–155.

[4]Butler, J. L., "Application Manual for the Design of EXTREMA Terfenol-D Magnetostrictive Transducers," Edge Technologies, Extrema Div., Ames, IA, 1989.

[5]Anastas, G., Eisenhaure, D., Hockney, R., Johnson, B., and Misovec, K., "Distributed Magnetic Actuators for Fine Shape Control," Air Force Astronautics Lab., AFAL-TR-88-026, Edwards AFB, CA, June 1988.

[6]Wayman, C. M., and Shimizu, K., "The Shape Memory ('Marmen') Effect in Alloys," *Metal Science Journal*, Vol. 6, 1972, pp. 175–183.

[7]Rogers, C. A., Liang, C., and Barker, D. K., "Dynamic Control Concepts Using Shape Memory Alloy Reinforced Plates," *Smart Materials, Structures and Mathematical Issues*, edited by C. A. Rogers, Technomic Publishing, Westport, CT, 1989.

[8]Coulter, J. P., Duclos, T. G., and Acker, D. N., "The Usage of Electrorheological Materials in Viscoelastic Layer Damping Applications," *Proceedings of the Damping '89 Conference*, Air Force Wright Aeronautical Lab., West Palm Beach, FL, Feb. 8–10, 1989, pp. CAA-1–CAA-17.

[9]Gandhi, M. V., and Thompson, B. S., "A New Generation of Revolutionary Ultra-Advanced Intelligent Composite Materials Featuring Electro-Rheological Fluids," *Smart Materials, Structures and Mathematical Issues*, edited by C. A. Rogers, Technomic Publishing, Westport, CT, 1989, pp. 63–68.

[10]Haftka, R. T., and Adelman, H. M., "An Analytical Investigation of Shape Control of Large Space Structures by Applied Temperatures," *AIAA Journal*, Vol. 23, No. 3, 1985, pp. 450–457.

[11]Edberg, D. L., "Control of Flexible Structures by Applied Thermal Gradients," *AIAA Journal*, Vol. 25, No. 6, 1987, pp. 877–883.

[12]Wada, B. K., Edberg, D., and Smith, G. R., "Adaptive Damping of Spacecraft by Temperature Control," *The Role of Damping in Vibration and Noise Control*, DE-Vol. 5, American Society of Mechanical Engineers, New York, 1987, pp. 89–92.

[13]Claus, R. O., McKeeman, J. C., May, R. G., and Bennett, K. D., "Optical Fiber Sensors and Signal Processing for Smart Materials and Structures Applications," *Smart Materials, Structures and Mathematical Issues*, edited by C. A. Rogers, Technomic Publishing, Westport, CT, 1989, pp. 29–38.

[14]Measures, R. M., "Smart Structures with Nerves of Glass," *Progress in Aerospace Sciences*, Vol. 26, No. 4, 1989, pp. 289–351.

[15]Parton, V. Z., and Kudryavtsev, B. A., *Electromagnetoelasticity*, Gordon & Breach, New York, 1988.

[16]"IEEE Standard on Piezoelectricity," Inst. of Electrical and Electronics Engineers, ANSI/IEEE Std 176-1987, New York, Jan. 1988.

[17]Wilson, E. G., "Static Aeroelasticity in the Design of Modern Fighters," *Static Aeroelasticity in Combat Aircraft*, AGARD Rept. 725, Nevilly Sur Seine, France, Jan. 1986.

[18]Crawley, E. F., Warkentin, D. J., and Lazarus, K. B., "Feasibility Analysis of Piezoelectric Devices," Space Systems Lab., Massachusetts Inst. of Technology, MIT-SSL-5-88, Cambridge, MA, Jan. 1988.

[19]Lazarus, K. B., Crawley, E. F., and Bohlmann, J. D., "Static Aeroelastic Control Using Strain Actuated Adaptive Structures," *Proceedings of the First Joint U.S./Japan Conference on Adaptive Structures*, Maui, HI, Oct. 1990, pp. 197–224.

[20]Ehlers, S. M., "Aeroelastic Behavior of an Adaptive Lifting Surface," Ph.D. Dissertation, School of Aeronautics and Astronautics, Purdue Univ., West Lafayette, IN, Aug. 1991.

[21]Song, O., Librescu, L., and Rogers, C. A., "Static Aeroelastic Behavior of Adaptive Aircraft Wing Structures Modelled as Composite Thin-Walled Beams," International Forum on Aeroelasticity and Structural Dynamics, Aachen, Germany, June 1991.

[22]Jones, R. M., *Mechanics of Composite Materials*, Scripta, Washington, DC, 1975.

[23]Barrett, R., "Intelligent Rotor Blade Actuation Through Directionally Attached Piezoelectric Crystals," American Helicopter Society Forum, Washington, DC, May 1990.

[24]Bisplinghoff, R. L., and Ashley, H., *Principles of Aeroelasticity*, Dover, New York, 1975.

[25]Weisshaar, T. A., "Aeroelastic Tailoring of Forward Swept Composite Wings," *Journal of Aircraft*, Vol. 18, No. 8, 1981, pp. 669–676.